Effect of an R69C Mutation in the Myelin Protein Zero Gene on Myelination and Ion Channel Subtypes

Yunhong Bai, MD; Emilia Ianokova, MD; Qin Pu, MD, PhD; Khaled Ghandour, BS; Rock Levinson, PhD;
Jean-Jacques Martin, MD; Chantal Ceuterick-de Groote, MD; Radim Mazanec, MD, PhD;
Pavel Seeman, MD, PhD; Michael E. Shy, MD; Jun Li, MD, PhD

Background: Most mutations in the myelin protein zero gene (*MPZ*) typically cause a severe demyelinating/dysmyelinating neuropathy that begins in infancy or an adult-onset axonal neuropathy. Axonal degeneration in the late-onset H10P mutation may be caused by the disruption of axoglial interaction.

Objective: To evaluate sural nerve biopsy samples from a patient with early-onset Charcot-Marie-Tooth disease type 1B caused by an arg69-to-cys (R69C) mutation.

Design and Participants: Biopsies of sural nerves were performed 20 years apart in a patient with an R69C mutation (early onset). In addition, peripheral nerves were obtained from autopsy material from a patient with a T95M mutation (late onset). These nerves were analyzed using light microscopy of semithin sections, teased nerve fiber immunohistochemical analysis, electron microscopy, and immunologic electron microscopy.

Main Outcome Measures: Pathological changes in sural nerve.

Results: Both R69C biopsy samples showed prominent demyelination and onion bulb formation, unlike the late-onset T95M mutation, which showed primarily axonal degeneration with no onion bulbs. The sural biopsy sample obtained 20 years earlier from the R69C patient showed minimal difference from the present sample, consistent with the lack of clinical progression during the 2 decades. Teased fiber immunohistochemical analysis of R69C revealed voltage-gated sodium channel subtype 1.8 expressions at the nodes of Ranvier around the areas of segmental demyelination. Internodal length in all R69C nerve fibers was invariably short (>94% of all internodes are <150 μm).

Conclusions: Morphologic abnormalities in this early-onset R69C neuropathy were severe in childhood but progressed very slowly after adolescence. The switch to voltage-gated sodium channel subtype 1.8 expression at the nodes may provide clues into the pathogenesis of this case of early-onset neuropathy, and the short internodes may contribute to the extremely slowed conduction velocities in this case (<10 m/s).

Arch Neurol. 2006;63:1787-1794

Author Affiliations:
Department of Neurology, Wayne State University School of Medicine, Detroit, Mich (Drs Bai, Ianokova, Pu, Shy, and Li and Mr Ghandour); Department of Physiology and Biophysics, School of Medicine, University of Colorado Health Science Center, Denver (Dr Levinson); Laboratory of Neuropathology, Born-Bunge Institute, and Department of Medicine, University of Antwerp, Antwerp, Belgium (Drs Martin and Ceuterick-de Groote); and Departments of Adult Neurology and Child Neurology, DNA Laboratory 2nd School of Medicine, Charles University Prague, Prague, Czech Republic (Drs Mazanec and Seeman).

THE MYELIN PROTEIN ZERO gene (*MPZ*) encodes a major myelin protein of 248 amino acids; the 29–amino acid signal peptide encoded by exon 1 is cleaved before the insertion of the final 219–amino acid protein into the myelin sheath. (Because the cleaved amino acids are not present in the myelin sheath, they are not included in the numbering of amino acids in this article. For example, R69C, T95M, and H10P would be R98C, T124M, and H39P as cited in the Inherited Peripheral Neuropathies Mutation Database available at: http://www.molgen.ua.ac.be/CMTMutations/default.cfm). The *MPZ* gene is expressed specifically by Schwann cells and mediates myelin compaction via homotypic adhesion that requires the extracellular and intracellular portions of the molecule.[1,2]

Mutations in the *MPZ* gene cause Charcot-Marie-Tooth disease type 1B (CMT1B)[3]; to date, more than 95 disease-causing *MPZ* mutations have been reported. We systematically examined the phenotypic presentation in CMT1B, and most patients in this study can be clustered into 2 phenotypic groups: one with onset of symptoms in infancy and a second with onset of symptoms in adulthood.[4] Early-onset patients have severely slow nerve conduction velocities (NCVs), typically less than 10 m/s. Alternatively, late-onset patients demonstrate axonal loss with NCVs greater than 30 m/s.

We recently performed an autopsy study on a patient with a late-onset form of CMT1B caused by an H10P mutation. The study demonstrated severe axonal degeneration with minimal segmental demyelination. Moreover, nerves from this patient also contained large accumulations of amorphous materials in the inner wraps of peripheral nerve myelin that may have disrupted Schwann cell–axon in-

teractions and caused the resultant axonal damage.[5] In the present study, we also examined autopsy material from another late-onset case of CMT1B, this one caused by a mutation in T95M.[6]

We now compared these results with pathologic findings from a patient with an early-onset form of CMT1B caused by an R69C mutation. R69C mutations have previously been shown to cause severe, early-onset neuropathies in several different patients.[7-9] Electron microscope (EM) studies from young patients have revealed regions of uncompacted myelin, 1 of 2 types of pathology previously reported in early-onset cases of CMT1B.[7,10,11] Previous R69C biopsy samples have also shown onion bulb formation, thinly myelinated axons,[8,12] and, on occasion, amyelinated fibers.[7,8] Teased fiber analysis has demonstrated demyelination and remyelination in patients with early-onset neuropathy.[12] Secondary axonal loss was frequent.[8,10,12,13]

However, despite these previously reported pathologic findings, little is known about the underlying pathogenic mechanisms in R69C or other cases of early-onset CMT1B. We had the opportunity to address this issue by evaluating a sural nerve biopsy sample from a patient with an R69C mutation that also caused a severe early-onset neuropathy. We evaluated disease progression morphologically by comparing our results with those from a sural nerve biopsy performed on the same patient 20 years earlier. Taken together, these results demonstrated that R69C caused significant segmental demyelination with a profound loss of large-diameter nerve fibers in early childhood. However, the axonal loss progressed only minimally during the next 20 years. We observed a change of voltage-gated sodium channel subtypes at the nodes of Ranvier, similar to what has been described in models of severe dysmyelinating neuropathies, such as Trembler[J] and *Mpz* knockout mice,[14,15] and in the brains of patients with multiple sclerosis.[16] Internodal length in all nerve fibers was very short (>94% of all internodes are <150 µm), which may significantly affect the NCVs.[17]

METHODS

A 45-year-old woman with an R69C heterozygous mutation of *MPZ* volunteered to donate her remaining sural nerve for scientific research. The nerve was cut into blocks and fixed immediately after removal from the patient. For semithin sections and EM, nerves were fixed in 2.5% glutaraldehyde overnight, osmicated for 1.5 hours, dehydrated, and embedded in epoxy resin. The semithin sections (1 µm thick) were stained with toluidine blue and were examined using a light microscope. The ultrathin sections were contrasted with lead citrate and uranyl acetate and were examined using an EM (Zeiss EM 900; Carl Zeiss Inc, Thornwood, NY). Blocks were also fixed in 0.5% glutaraldehyde and 4% paraformaldehyde for 3 hours and embedded in LR-white resin for immunologic EM. A sural nerve sample from a biopsy performed 20 years earlier on the same patient, embedded in Epon, was also analyzed. At that time, no genetic test was available, and the sural nerve biopsy was performed to aid in her diagnosis.

For immunohistochemical analysis, blocks were fixed in 4% paraformaldehyde for 15 minutes or were freshly frozen in OCT medium. Nerves were teased into individual fibers on glass slides.

The slides were dried overnight, reacted with primary antibodies the following day, and kept at 4°C overnight, followed by 2-hour incubation with secondary antibodies. The stained slides were examined using a fluorescent microscope (Leica Microsystems, Wetzlar, Germany). The following antibodies were used: rat monoclonal antibodies to MBP (1:500) (Chemicon International Inc, Temecula, Calif), mouse monoclonal antibodies to MPZ (1:50),[18] mouse monoclonal and rabbit polyclonal antibodies to Caspr (1:500),[19] mouse monoclonal anti-Kv1.2 (1:100) (Upstate Biotechnology, Chicago, Ill), rabbit and mouse monoclonal antibodies to pan voltage-gated sodium channels (Na$_v$) (1:500) (Sigma-Aldrich Corp, St Louis, Mo), and rabbit monoclonal antibodies to voltage-gated sodium channel subtype 1.8 (Na$_v$1.8)[20] and CD68 (1:500) (Dako, Carpinteria, Calif). The Na$_v$1.8 antibodies were initially characterized and reported with a previously used nomenclature of α-SNS/PN3.[20]

For morphometric analysis, semithin sections (thickness=1 µm) were examined under a 63× objective. Each consecutive field was captured using a charged coupled device digital camera. Images were imported into morphometric software (Image-Pro Plus; Media Cybernetics Inc, Silver Spring, Md). Areas of each field were counted to obtain nerve fiber density, myelin thickness, g-ratio, and histograms.

An 89-year-old man carried a T95M heterozygous mutation of *MPZ* (late onset). An autopsy was completed within 12 hours of his death. Sciatic, tibial, ulnar, and sural nerves were harvested for light microscope and EM examination. All the studies were approved by the institutional review board of Charles University, and appropriate consent was obtained by the local physicians who performed the biopsies or autopsies.

RESULTS

CASE PRESENTATIONS

The clinical course of the patient with the R69C mutation was previously reported in the Czech literature.[21] This 45-year-old woman was hypotonic in infancy, with delayed motor milestones. She never achieved normal independent gait. However, her neurologic function remained stable, without further clinical progression, since adolescence. Nerve conduction studies showed markedly slowed NCVs (<10 m/s) in all the nerves that were recordable. Compound muscle amplitude potentials were significantly reduced in the arms and absent in the legs. Sensory nerve action potentials were absent in the arms and legs.

The clinical presentation of the T95M patient has already been reported,[6] as has the late-onset H10P patient whose nerves we used for the sodium channel immunohistochemical analysis in the present study.[5] Both had a late-onset sensorimotor neuropathy with electrophysiologic features most characteristic of axonal degeneration.

MILD PATHOLOGIC PROGRESSION IN 20 YEARS IN R69C SURAL NERVES

Sural nerve recently obtained from the R69C patient showed numerous "onion bulbs" and severe loss of large-diameter myelinated nerve fibers (**Figure 1**). Surviving myelinated nerve fibers were small (<8 µm in diameter) (Figure 1). These findings were characteristic of a chronic demyelinating/dysmyelinating process with secondary axonal degeneration. We then reanalyzed the sural nerve sample from the biopsy performed 20 years ago,
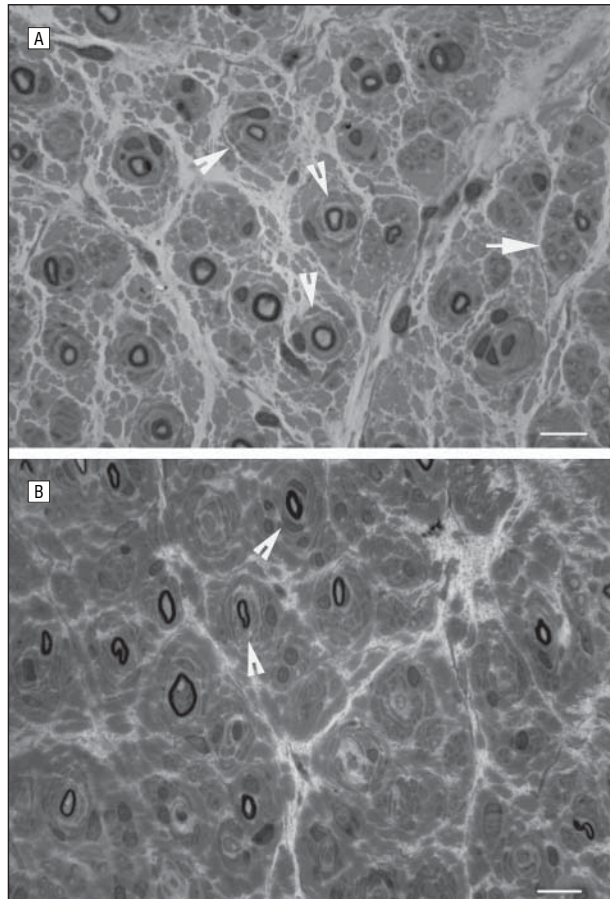
Figure 1. Pathologic features in the R69C sural nerve (toluidine blue). A, Semithin section of a sural nerve biopsy of R69C performed 20 years previously. Almost all the myelinated nerve fibers form onion bulbs (arrowheads). These features suggest chronic demyelination and remyelination. The arrow points to a cluster of tiny nerve fibers that could be regenerating nerves. There is severe loss of large-diameter myelinated fibers. The surviving myelinated fibers appear small in diameter. B, Semithin biopsy section of the other sural nerve, obtained recently, shows pathologic changes and axonal loss similar to those observed in the sural nerve 20 years previously. Scale bars=10 µm.
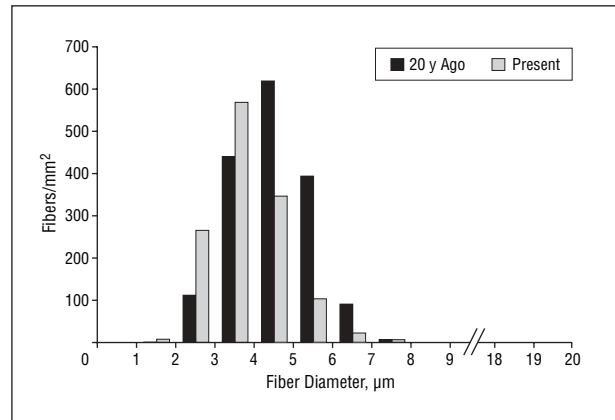

Figure 2. Minimal pathologic progression in 20 years in the R69C sural nerves. Sural nerves of R69C were morphometrically analyzed and were plotted as a histogram. Myelinated nerve fibers larger than 8 µm in diameter were not found. The quantity and distribution of myelinated nerve fibers are only minimally different from the findings obtained 20 years previously.
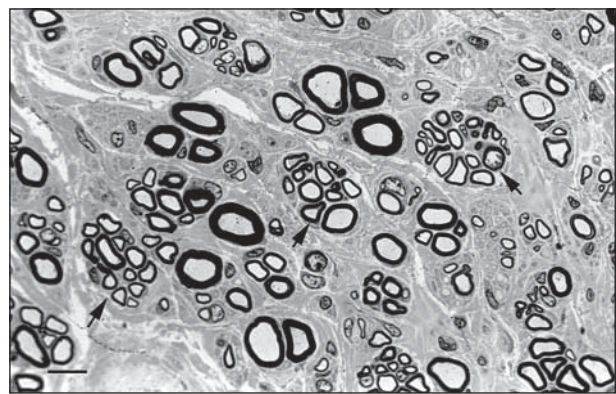

Figure 3. Pathologic features of the T95M autopsy nerve. A semithin section obtained from the ulnar nerve of T95M shows severe axonal loss and regenerative clusters (arrows), typical features of axonal degeneration (toluidine blue). No onion bulbs are visible. Scale bar=10 µm.

from the contralateral leg, and compared the findings with those from the recent biopsy. Nerve fiber densities in the 2 nerves appeared nearly identical (Figure 1). To quantitatively evaluate the axonal loss, we performed morphometric analysis on the 2 biopsy samples. The result showed only a minimal change between the sural nerve obtained 20 years ago and the present nerve (1668 vs 1315 fibers/µm^2) (**Figure 2**). Thus, pathologic progression of the neuropathy was small. These findings are consistent with the clinical observation that this patient had a stable neurologic deficit for 2 decades after the initial deterioration during the first decade of her life.

MORPHOLOGIC FEATURES ARE DISTINCT FROM LATE-ONSET CMT1B CAUSED BY T95M

To compare the previous findings with those from a late-onset patient with CMT1B, we analyzed peripheral nerves from a patient with a T95M mutation. Unlike R69C, onion bulbs were not observed in T95M, whereas regenerating clusters of small-diameter fibers were common (arrowheads in **Figure 3**). As with R69C, large-diameter nerve fibers were scarce. These features were found in all the nerves evaluated and confirmed other reports that T95M caused a severe axonal neuropathy.[6,22-24]

These findings were also similar to those observed in another late-onset form of CMT1B caused by an H10P mutation.[5] In this H10P autopsy, we identified extensive proteinaceous inclusions in the inner intralaminar or periaxonal space, particularly in the dorsal roots. We did not have roots to evaluate from the T95M autopsy. However, we identified 2 myelinated fibers from the T95M sciatic nerve that contained a large amount of vesicular material in the periaxonal space.

Morphometric analysis was performed on sural and sciatic nerves from the T95M patient. Large-diameter myelinated nerve fibers (>12 µm) were absent in sural and sciatic nerves, consistent with severe axonal loss of large-diameter myelinated fibers (**Figure 4**).

SEGMENTAL DEMYELINATION IN R69C BUT NOT IN T95M

To reliably evaluate segmental demyelination we performed teased fiber analysis on the recent R69C sural nerve biopsy sample. Segmental demyelination was common
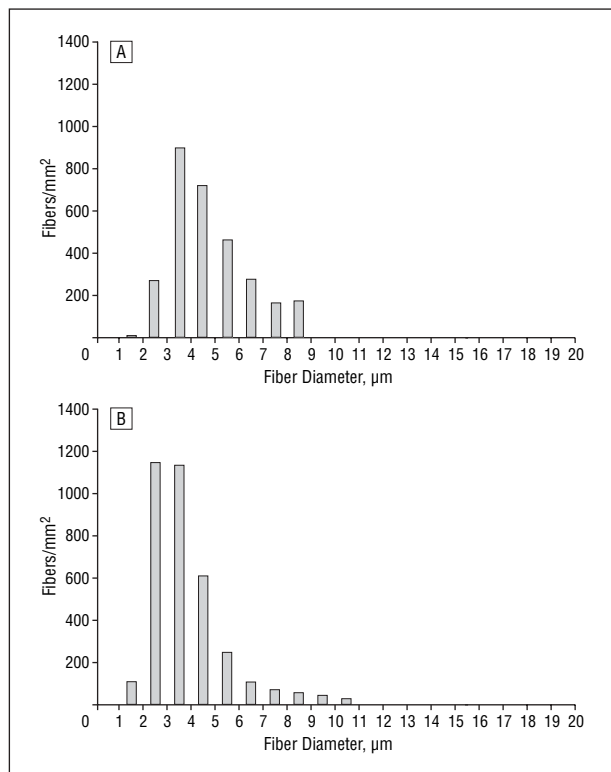
Figure 4. Severe axonal loss in the T95M autopsy nerves. Sural (A) and sciatic (B) nerves of T95M were morphometrically analyzed and were plotted as a histogram. Myelinated nerve fibers larger than 12 µm in diameter are absent, suggesting severe loss of large-diameter nerve fibers in the patient with a T95M mutation.

(**Figure 5**A). Macrophages were also detected in demyelinated areas, although only in less than 2% of nerve fibers. No material was available for teased fiber analysis in the T95M autopsy that was performed many years earlier. However, previous studies[22,23] on patients with T95M mutation have shown severe axonal degeneration with no segmental demyelination on teased nerve fiber preparations and semithin sections, although 1 study[24] noted a few thinly myelinated fibers that were interpreted as signs of remyelination. Taken together, these findings demonstrate that the R69C mutation causes a pathologic phenotype that, like the clinical phenotype, is distinct from that of the T95M mutation.

SHORT INTERNODES IN R69C

Internodal length in sural nerves in healthy controls younger than 60 years varies with nerve fiber diameters but is never less than 150 µm.[25,26] The internodal lengths of sural nerve fibers from the R69C biopsy, however, were consistently less than 150 µm. We randomly selected and measured 50 internodes on teased fiber preparation. Only 3 (6%) of 50 internodes were longer than 150 µm. The mean±SD internodal length was 120±23 µm, which was, therefore, abnormally short. In more than 50% of the fibers the internodal length was variable, suggesting that there had been demyelination followed by remyelination (Figure 5B and C). However, the remaining fibers exhibited consecutive uniformly short internodes (5-8 internodes in the row), with symmetrical paranodes, not

typical of internodes that had undergone demyelination and remyelination. These results suggest that internodes in these fibers have never reached the normal length in development and thus may represent a dysmyelinating abnormality (Figure 5D and E).

Contact between the myelin sheath and the underlying axolemma is necessary for the normal clustering of axolemmal proteins, such as sodium channels in nodes of Ranvier, potassium channels in juxtaparanodes, and Caspr in paranodes.[27,28] Because the localization of these molecules is disrupted in several animal models of demyelinating neuropathy,[15,29] we investigated whether their distribution was altered in the recent R69C biopsy sample. In regions of segmental demyelination, Caspr was no longer localized to paranodes but was spread into demyelinated regions of sural nerve axons (Figure 5F), as reported in animal models of segmental demyelination.[15,28,29] In contrast, Caspr remained discrete and symmetrical in the uniformly short internodal regions without segmental demyelination (Figure 5E).

Na$_v$1.8 EXPRESSION IN DEMYELINATED INTERNODES IN R69C

Voltage-gated sodium channels have been shown to switch from subtype 1.6 to subtype 1.8 at nodes of Ranvier in a series of animal models of demyelinating or dysmyelinating neuropathies, such as in *Mpz* knockout mice[14] and Trembler^J (PMP22 missense mutation) mice.[15] To determine whether a similar switch occurred in CMT1B, we performed similar studies on teased fibers from the sural nerve biopsy sample from the R69C patient. These antibodies against Na$_v$1.8 have been characterized and used in previous publications.[14,20] Of 180 randomly encountered nodes, 38 (21%) were stained with Na$_v$1.8 antibodies. The nodes with Na$_v$1.8 expression were found only in areas of segmental demyelination but not in nodes from regions of consecutive uniformly short internodes (Figure 5B and C). In particular, heminodes at the edges of remyelinating Schwann cells expressed Na$_v$1.8 (Figure 5B), a phenomenon reminiscent of the expression pattern of Na$_v$1.2 during development and remyelination.[27,30,31] Preabsorption of anti–Na$_v$1.8 antibodies with specific antigen peptide abolished the staining of Na$_v$1.8. We did not have material from the T95M autopsy for immunohistochemical analysis. Therefore, we used previously frozen nerves from an H10P autopsy, which we have also shown causes a late-onset axonal neuropathy,[5] and analyzed Na$_v$1.8 expression in these nerves. One hundred nodes in the H10P nerves were randomly counted, and only 4% of these nodes were stained by the Na$_v$1.8 antibodies. In contrast, all the nodes on the teased fibers of H10P were labeled by antibodies against pan-Na$_v$. Thus, Na$_v$1.8 expression seemed to be predominantly limited to demyelinating/remyelinating internodes in the R69C patient.

NORMAL MYELIN COMPACTION IN R69C

Previous studies[7] of severe early-onset CMT1B, including cases of R69C, have demonstrated either abnormalities of myelin compaction or the formation of tomaculi
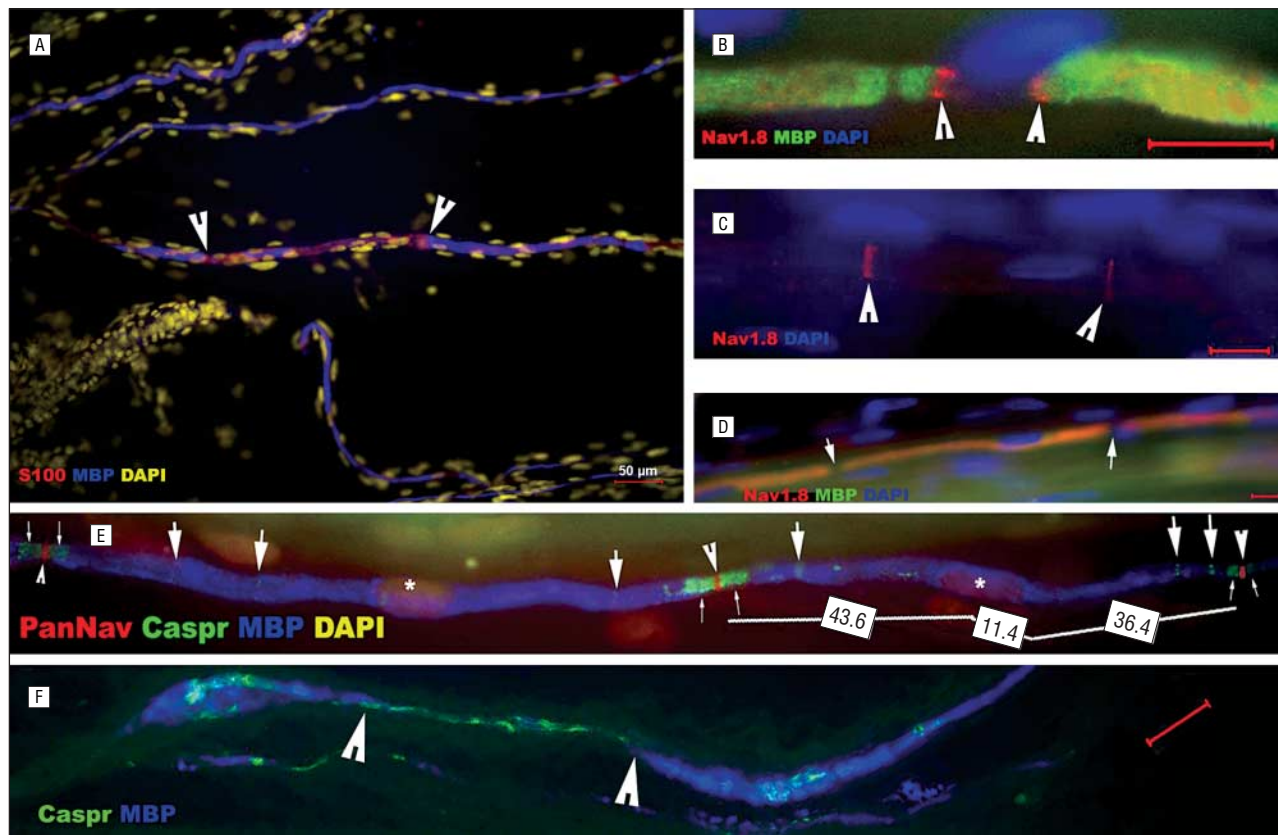
Figure 5. Segmental demyelination and voltage-gated sodium channel subtype 1.8 (Na$_v$1.8) expression in the sural nerve biopsy sample. Sural nerve from the patient with the R69C mutation was teased into individual nerve fibers and immunostained. A, A teased myelinated nerve fiber was double-stained with antibodies against the myelin protein myelin basic protein (MBP) (blue) and the Schwann cell protein S100 (red). The region with absent MBP staining (between the arrowheads) indicates segmental demyelination, which was common in this biopsy sample. 4′,6-Diamidino-2-phenylindole (DAPI)–labeled nuclei (yellow) were numerous and suggested an increased number of Schwann cells. Cells containing these nuclei were not stained with antibodies to the macrophage marker CD68. B, A teased myelinated nerve fiber was double-stained with antibodies against MBP (green) and Na$_v$1.8 (red). The Na$_v$1.8 forms heminodes at the borders of remyelinating Schwann cells (arrowheads). C, A remyelinated short internode (approximately 35 μm long) is flanked by 2 nodes with expression of Na$_v$1.8 (arrowheads). D and E, Some nerve fibers (approximately 50%) contain consecutive uniformly short internodes (5-8 internodes in the row) with no evidence of segmental demyelination. Nodes of Ranvier (arrows) in these nerve fibers have no detectable Na$_v$1.8. However, these nodes can be labeled with antibodies against pan Na$_v$ (red, arrowheads in part E). In addition, paranodes stained with anti–Caspr antibodies are symmetrical (green, small arrows in part E) in these areas of nerve fibers with several consecutive uniform short internodes (usually 5-8 internodes in the row). Schmidt-Lantermann incisures are also labeled with Caspr (large arrows in part E). Asterisks mark the Schwann cell nuclei in a ratio of 1 nucleus per internode. Note that the Schwann cell nucleus on the left is slightly eccentrically placed. The significance of this eccentricity is unclear. The numbers showing drawn distances give an estimation of internodal length. F, Teased nerve fibers were double-stained with antibodies against MBP and Caspr. The absence of MBP (blue) in the middle of a myelinated nerve fiber (between the arrowheads) is conspicuous, suggesting segmental demyelination. Unlike the nondemyelinated nerve fiber in part E, the paranodal marker Caspr (green) is no longer confined to the paranodal region; instead, it becomes irregular and spreads into the entire demyelinated region. Scale bars indicate 10 μm (B-D) and 20 μm (F).

in sural nerve biopsy samples. We found no abnormalities of myelin compaction in either of the R69C biopsy samples. We also did not observe focal swellings of misfolded myelin suggestive of tomaculi.

MPZ EXPRESSION IN COMPACT MYELIN WAS NOT REDUCED BY R69C

Mutant MPZ has been hypothesized to interfere with intracellular protein trafficking and reduce the amount of MPZ available to be incorporated into the myelin sheath.[13] We, therefore, used immunologic EM to determine whether the R69C mutation reduced MPZ levels in myelinated fibers of our patient's sural nerve. Myelinated nerves from skin biopsy samples of healthy controls were used. This technique was established by us previously and successfully detected changes in PMP22 levels in patients with *PMP22* gene duplication or deletion.[32] We found that the amount of MPZ expression in R69C nerves

was almost identical to that of the control (**Figure 6**), suggesting that MPZ reaches a normal amount on the myelin of R69C nerves. However, with this assay we could not determine the extent to which the mutant allele contributed to the level of MPZ in compact myelin.

COMMENT

This study demonstrates a distinct pathologic mechanism for the early-onset form of CMT1B caused by an R69C mutation compared with that in late-onset CMT1B caused by T95M and H10P mutations. Thus, the results are consistent with the distinct clinical phenotypes of early- and late-onset *MPZ* mutations previously described.[4] We recognize that these results are from individual patients and may not represent all cases of early- or late-onset CMT1B. However, the clinical and physiologic phenotypes of the R69C and T95M patients
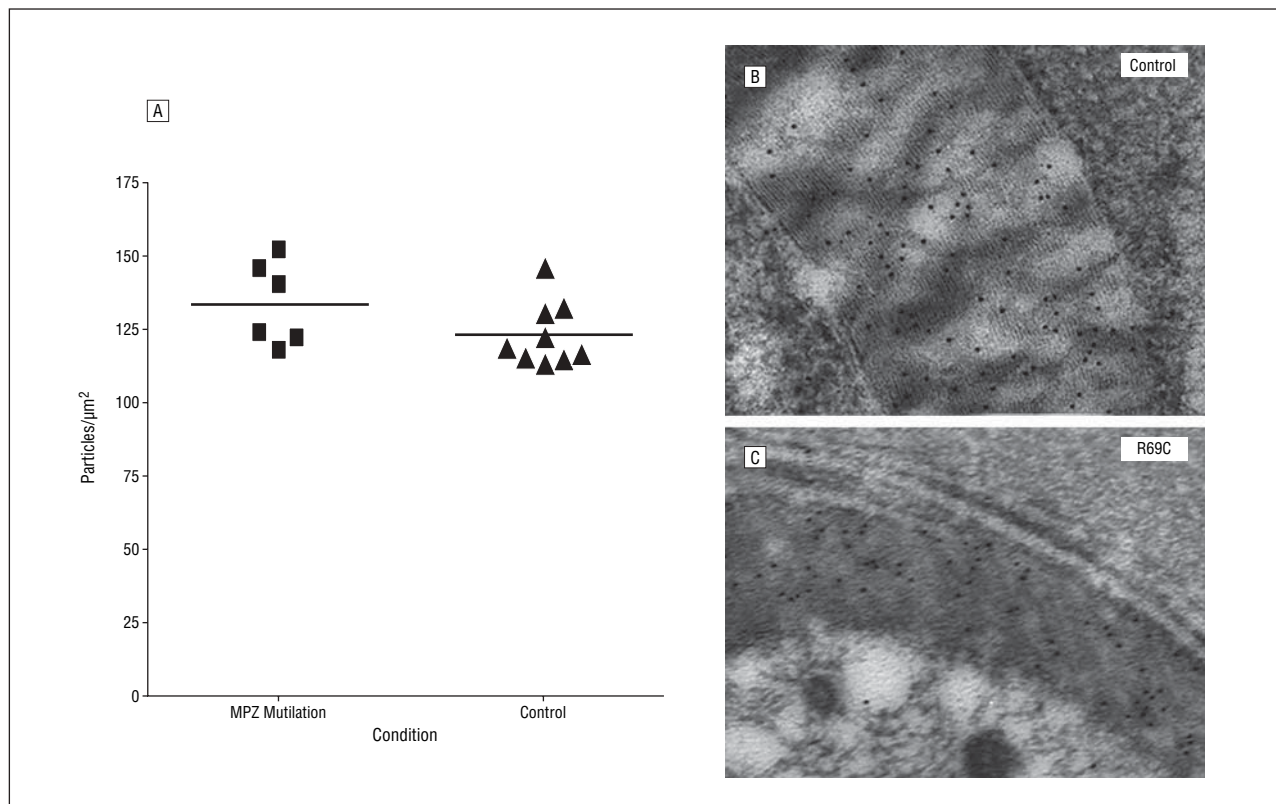
Figure 6. Expression of myelin protein zero (MPZ) in R69C sural nerve myelin is not reduced. A, The density of MPZ was quantified per area in the myelin. There was no significant difference in MPZ density between the control and R69C ($P>.05$). Each data point represents the mean MPZ density from a myelinated nerve fiber. The MPZ was labeled with antibodies conjugated with gold particles in a normal dermal myelinated nerve fiber (B) and a nerve fiber from an R69C sural nerve (C).The control subject had no history of peripheral nerve disease. The skin biopsy sample was obtained from the lateral side of the index finger using a previously established technique.[32]

we describe are typical of others reported in the literature with these identical mutations (reviewed by Shy et al[4]). To understand the pathogenic mechanisms of CMT1B it will be necessary to determine whether other patients with the same or another early- or late-onset neuropathy will have similar pathologic abnormalities and alterations of the molecular architecture of myelinated nerves. Therefore, we believe it is important to report these findings, particularly given the difficulty in obtaining sural nerve biopsy samples when they are no longer needed for diagnosis.

Sural nerves from the R69C patient showed conspicuous segmental demyelination and onion bulb formation. In contrast, T95M and H10P late-onset mutations caused severe axonal degeneration with no or minimal segmental demyelination. These late-onset pathologic abnormalities are also distinct from those described in *Mpz* heterozygous knockout mice, whose neuropathy is caused by a loss of MPZ function.[33,34] These mice develop an adult-onset neuropathy but with slow NCV and evidence of segmental demyelination accompanied by inflammatory cells.[33] Thus, the present T95M and H10P cases seem to be caused by an abnormal gain of function by the mutant MPZ rather than the simple loss of normal MPZ function. At present, no transgenic animal models of R69C, H10P, or T95M are available. Because it is unrealistic to make animal models for all 95 known *MPZ* mutations, careful reporting of morphologic material from patients will be important to identify the gain of function pathways in question.

The R69C patient had minimal disease progression in adulthood despite having severe impairment in early childhood. She was hypotonic in infancy, had delayed motor milestones, and never achieved normal independent gait. Findings from her 2 sural nerve biopsies were consistent with her lack of clinical progression between the teenage years and her present age. Morphometric analysis revealed only minimal changes in the number and sizes of myelinated fibers in both biopsies. Although we cannot prove this, our results suggest that much of the morphologic change in the sural nerve had been completed by the time the first biopsy was performed. The sural nerve biopsy on the same mutation reported by Gabreels-Festen and colleagues[7] was on a 14-month-old infant, also with a severe early-onset neuropathy. In this biopsy sample, more than 20% of the myelinated axons were poorly compacted, a finding not observed in either of the biopsy specimens from the present patient. In the Gabreels-Festen biopsy the myelinated fiber density was 46% of control values compared with only 20% to 22% in the present biopsy of R69C. Although it is possible that these differences reflect distinct pathologic and pathogenic mechanisms between the 2 patients, we believe that it is more likely that the differences simply reflect the disease progression during childhood. We hypothesize that the R69C patient may have had abnormalities in myelin compaction in infancy but that these abnormalities of compaction disappeared with age. Perhaps poorly compacted myelin predisposed large-diameter axons to de-

generate. The remaining small myelinated nerve fibers might have been more resistant to axonal degeneration and thus been the fibers that remain in adulthood. The paucity of macrophages observed in the R69C biopsies may reflect the indolent nature of the process in adulthood.

Another insight into the potential pathogenesis of this R69C neuropathy comes from the presence of the shortened internodes of less than 150 μm in the biopsy findings of the nerve fibers. A previous study[35] using mathematical modeling suggested that short internodes may cause slowing of NCVs. Court and colleagues[17] demonstrated that uniformly shortened internodes in young periaxin null mice were sufficient to reduce NCVs to 10 m/s, even when axonal diameters and myelin thickness were normal, before demyelination occurred. These data suggest that in the R69C mutation, short internodes alone may be sufficient to cause the NCV of less than 10 m/s observed by us and others. [7,8]

Previously, NCVs in the range of 10 m/s were thought to result from severe segmental demyelination and remyelination.[36] Although demyelination and remyelination were observed in the present biopsy samples, it is not clear whether these processes alone could account for the severe slowing observed in R69C. Segmental demyelination and remyelination are characteristic features of acquired demyelinating neuropathies, such as Guillain-Barre syndrome and chronic inflammatory demyelinating polyneuropathy.[37] In these disorders it is rare to have NCVs as low as 10 m/s. Similarly, it is unlikely that a loss of large-diameter axons could account for the slow NCVs seen in these patients. Severe loss of large-diameter nerve fibers was also seen in the present autopsies with late-onset *MPZ* mutations (T95M and H10P), but the NCVs in these 2 patients were only slightly reduced (approximately 40 m/s).[5,6]

A final point of discussion is the significance of the $Na_v1.8$ expression at the nodes of Ranvier in demyelinating/remyelinating regions (Figure 5). To our knowledge, this is the first time that such subtype switching of ion channels has been described in human peripheral nerve. Similar findings, however, have been reported in 2 neuropathy animal models with chronic demyelination/dysmyelination, including *Mpz* knockout and Trembler[J] mice[14,15] and in brains from patients with multiple sclerosis.[16] Because we noted $Na_v1.8$ expression in regenerating heminodes and nodes in remyelinating regions, it seemed reasonable to predict that $Na_v1.8$ channel expression may be involved in the process of remyelination. Because $Na_v1.8$ possesses different electrophysiologic properties than $Na_v1.6$,[38,39] it also seems reasonable to speculate that $Na_v1.8$ expression at nodes of Ranvier may contribute to alterations in axonal excitability. Axonal excitability change has been documented in patients with CMT1A,[40] in whom nerve abnormality is similar to that in Trembler[J] mice, which have a PMP22 missense mutation and $Na_v1.8$ expression.[15] It will be interesting to determine whether $Na_v1.8$ expression is also expressed in nerves from patients with other inherited demyelinating neuropathies, such as CMTX.

In summary, we show that the R69C *MPZ* mutation causes a severe early-onset neuropathy that seems to slowly progress clinically and pathologically after adolescence. Pathologic abnormalities demonstrate a marked loss of large-diameter axons along with prominent segmental demyelination and remyelination. In addition, strikingly short internodes may contribute to extremely slow NCVs. We identified a switch in Na_v subtypes, but only in areas undergoing demyelination and remyelination. These findings are distinct from those found in late-onset CMT1B caused by a T95M (and an H10P) mutation in which there was only minimal demyelination and $Na_v1.8$ expression, whereas marked disease progression occurred during adulthood.

REFERENCES

1. Shapiro L, Doyle JP, Hensley P, Colman DR, Hendrickson WA. Crystal structure of the extracellular domain from P₀, the major structural protein of peripheral nerve myelin. *Neuron*. 1996;17:435-449.
2. Filbin MT, Zhang K, Li W, Gao Y. Characterization of the effect on adhesion of different mutations in myelin P₀ protein. *Ann N Y Acad Sci*. 1999;883:160-167.
3. Hayasaka K, Takada G, Ionasescu VV. Mutation of the myelin P0 gene in Charcot-Marie-Tooth neuropathy type 1B. *Hum Mol Genet*. 1993;2:1369-1372.
4. Shy ME, Jani A, Krajewski K, et al. Phenotypic clustering in MPZ mutations. *Brain*. 2004;127:371-384.
5. Li J, Bai YH, Ianakova E, et al. Major myelin protein gene (P0) mutation causes a novel form of axonal degeneration. *J Comp Neurol*. 2006;498:252-265.
6. De Jonghe P, Timmerman V, Ceuterick C, et al. The Thr124Met mutation in the peripheral myelin protein zero (MPZ) gene is associated with a clinically distinct Charcot-Marie-Tooth phenotype. *Brain*. 1999;122:281-290.
7. Gabreels-Festen AA, Hoogendijk JE, Meijerink PH, et al. Two divergent types of nerve pathology in patients with different P0 mutations in Charcot-Marie-Tooth disease. *Neurology*. 1996;47:761-765.
8. Komiyama A, Ohnishi A, Izawa K, Yamamori S, Ohashi H, Hasegawa O. De novo mutation (Arg⁹⁸→Cys) of the myelin P₀ gene and uncompaction of the major dense line of the myelin sheath in a severe variant of Charcot-Marie-Tooth disease type 1B. *J Neurol Sci*. 1997;149:103-109.
9. Warner LE, Hilz MJ, Appel SH, et al. Clinical phenotypes of different MPZ (P0) mutations may include Charcot-Marie-Tooth type 1B, Dejerine-Sottas, and congenital hypomyelination. *Neuron*. 1996;17:451-460.

10. Marrosu MG, Vaccargiu S, Marrosu G, Vannelli A, Cianchetti C, Muntoni F. Charcot-Marie-Tooth disease type 2 associated with mutation of the myelin protein zero gene. *Neurology*. 1998;50:1397-1401.

11. Meijerink PH, Hoogendijk JE, Gabreels-Festen AA, et al. Clinically distinct codon 69 mutations in major myelin protein zero in demyelinating neuropathies. *Ann Neurol*. 1996;40:672-675.

12. Ikegami T, Nicholson G, Ikeda H, et al. A novel homozygous mutation of the myelin Po gene producing Dejerine-Sottas disease (hereditary motor and sensory neuropathy type III). *Biochem Biophys Res Commun*. 1996;222:107-110.

13. Shames I, Fraser A, Colby J, Orfali W, Snipes GJ. Phenotypic differences between peripheral myelin protein-22 (PMP22) and myelin protein zero (P0) mutations associated with Charcot-Marie-Tooth-related diseases. *J Neuropathol Exp Neurol*. 2003;62:751-764.

14. Ulzheimer JC, Peles E, Levinson SR, Martini R. Altered expression of ion channel isoforms at the node of Ranvier in P0-deficient myelin mutants. *Mol Cell Neurosci*. 2004;25:83-94.

15. Devaux JJ, Scherer SS. Altered ion channels in an animal model of Charcot-Marie-Tooth disease type IA. *J Neurosci*. 2005;25:1470-1480.

16. Black JA, Dib Haijj S, Baker D, Newcombe J, Cuzner ML, Waxman SG. Sensory neuron-specific sodium channel SNS is abnormally expressed in the brains of mice with experimental allergic encephalomyelitis and humans with multiple sclerosis. *Proc Natl Acad Sci U S A*. 2000;97:11598-11620.

17. Court FA, Sherman DL, Pratt T, et al. Restricted growth of Schwann cells lacking Cajal bands slows conduction in myelinated nerves. *Nature*. 2004;431:191-195.

18. Archelos JJ, Roggenbuck K, Schneider-Schaulies J, Linington C, Toyka KV, Hartung HP. Production and characterization of monoclonal antibodies to the extracellular domain of P0. *J Neurosci Res*. 1993;35:46-53.

19. Peles E, Nativ M, Lustig M, et al. Identification of a novel contactin-associated transmembrane receptor with multiple domains implicated in protein-protein interactions. *EMBO J*. 1997;16:978-988.

20. Gould HJ III, Gould TN, England JD, Paul D, Liu ZP, Levinson SR. A possible role for nerve growth factor in the augmentation of sodium channels in models of chronic pain. *Brain Res*. 2000;854:19-29.

21. Seeman P, Mazabenc R, Horacek O, et al. Divergentni fenotypy choroby Charcot-Marie-Tooth: demyelinizacni s infantilnim zacatkem a axonalni s pozdnim zacatkem a zpomalenou fotoreakci nasledkem ruznych mutaci myelin protein zero. *Ceská a Slovenská Neurol Neurochirurg*. 2004;67:321-329.

22. Chapon F, Latour P, Diraison P, Schaeffer S, Vandenberghe A. Axonal phenotype of Charcot-Marie-Tooth disease associated with a mutation in the myelin protein zero gene. *J Neurol Neurosurg Psychiatry*. 1999;66:779-782.

23. Hanemann CO, Gabreels-Festen AA, De Jonghe P. Axon damage in CMT due to mutation in myelin protein P0. *Neuromuscul Disord*. 2001;11:753-756.

24. Mastaglia FL, Nowak KJ, Stell R, et al. Novel mutation in the myelin protein zero gene in a family with intermediate hereditary motor and sensory neuropathy. *J Neurol Neurosurg Psychiatry*. 1999;67:174-179.

25. Jacobs JM. On internodal length. *J Anat*. 1988;157:153-162.

26. Jacobs JM, Love S. Qualitative and quantitative morphology of human sural nerve at different ages. *Brain*. 1985;108:897-924.

27. Rasband MN, Kagawa T, Park EW, Ikenaka K, Trimmer JS. Dysregulation of axonal sodium channel isoforms after adult-onset chronic demyelination. *J Neurosci Res*. 2003;73:465-470.

28. Rasband MN, Trimmer JS, Schwarz TL, et al. Potassium channel distribution, clustering, and function in remyelinating rat axons. *J Neurosci*. 1998;18:36-47.

29. Neuberg DH, Sancho S, Suter U. Altered molecular architecture of peripheral nerves in mice lacking the peripheral myelin protein 22 or connexin32. *J Neurosci Res*. 1999;58:612-623.

30. Rasband MN, Trimmer JS. Developmental clustering of ion channels at and near the node of Ranvier. *Dev Biol*. 2001;236:5-16.

31. Craner MJ, Lo AC, Black JA, Waxman SG. Abnormal sodium channel distribution in optic nerve axons in a model of inflammatory demyelination. *Brain*. 2003;126:1552-1561.

32. Li J, Bai Y, Ghandour K, et al. Skin biopsies in myelin-related neuropathies: bringing molecular pathology to the bedside. *Brain*. 2005;128:1168-1177.

33. Shy ME, Arroyo E, Sladky J, et al. Heterozygous P0 knockout mice develop a peripheral neuropathy that resembles chronic inflammatory demyelinating polyneuropathy (CIDP). *J Neuropathol Exp Neurol*. 1997;56:811-821.

34. Martini R, Mohajeri MH, Kasper S, Giese KP, Schachner M. Mice doubly deficient in the genes for P0 and myelin basic protein show that both proteins contribute to the formation of the major dense line in peripheral nerve myelin. *J Neurosci*. 1995;15:4488-4495.

35. Brill MH, Waxman SG, Moore JW, Joyner RW. Conduction velocity and spike configuration in myelinated fibers: computed dependence on internode distance. *J Neurol Neurosurg Psychiatry*. 1977;40:769-774.

36. Waxman SG, Craner MJ, Black JA. Na+ channel expression along axons in multiple sclerosis and its models. *Trends Pharmacol Sci*. 2004;25:584-591.

37. Albers JW, Kelly JJ Jr. Acquired inflammatory demyelinating polyneuropathies: clinical and electrodiagnostic features. *Muscle Nerve*. 1989;12:435-451.

38. Leffler A, Herzog RI, Dib-Hajj SD, Waxman SG, Cummins TR. Pharmacological properties of neuronal TTX-resistant sodium channels and the role of a critical serine pore residue. *Pflugers Arch*. 2005;451:454-463.

39. Craner MJ, Kataoka Y, Lo AC, Black JA, Baker D, Waxman SG. Temporal course of upregulation of Na(v)1.8 in Purkinje neurons parallels the progression of clinical deficit in experimental allergic encephalomyelitis. *J Neuropathol Exp Neurol*. 2003;62:968-975.

40. Nodera H, Bostock H, Kuwabara S, et al. Nerve excitability properties in Charcot-Marie-Tooth disease type 1A. *Brain*. 2004;127:203-211.

Announcement

Visit www.archneurol.com. As an individual subscriber to *Archives of Neurology*, you have full-text online access to the journal from 1998 forward. In addition, you can find abstracts to the journal as far back as 1975.